COBEM 2021 Florianópolis - Brasil
26th ABCM International Congress of Mechanical Engineering
November 22-26, 2021. Florianópolis, SC, Brazil

WAYPOINT-BASED GUIDANCE FOR MULTIROTOR AERIAL VEHICLES USING ADAPTIVE GLOBAL SLIDING MODES

Luiz Gustavo Pereira Roéfero
Jorge Antonio Ricardo Jr
Davi A. dos Santos
Aeronautics Institute of Technology, Praça Mal. Eduardo Gomes, 50 - Vila das Acácias, São José dos Campos - SP, 12228-900, Brazil
roefero@ita.br
jorgejarj@ita.br
davists@ita.br

Abstract. *The present paper investigates the waypoint-based guidance of an under-actuated multirotor aerial vehicle (MAV) subject to bounded disturbances with unknown bounds. To address the problem, we adopt a hierarchical control structure, in which the attitude and position control loops are nested inside an outer-loop guidance. A reduced-order closed-loop dynamic model describing the inner control loops is obtained on the basis of a translation-rotation time-scale separation assumption and considering the use of inverse dynamic stabilizing position and attitude control laws. This model represents the dynamics of the stabilized heading and three-dimensional position, which are the four trackable degrees of freedom of an under-actuated MAV. The afore-described model is employed in the design of the guidance law using a multivariable adaptive global sliding mode control (AGSMC) technique. In particular, to effectively guarantee a global sliding motion, the switching-gain adaptation law is designed to be monotonically increasing. The proposed method is evaluated using numerical simulation, which verifies its effectiveness to robustly guide a vehicle, under completely unknown disturbances, along a specified waypoint sequence.*

Keywords: *sliding mode control, multirotor aerial vehicle, waypoint-based guidance.*

1. INTRODUCTION

Thanks to their good maneuverability, vertical takeoff and landing capability, and relative simplicity, multirotor aerial vehicles (MAV) have recently attracted interest for critical urban-air-mobility applications, such as air taxi (Rajendran and Srinivas, 2020) and delivery (Park *et al.*, 2016). In many of these tasks, it is interesting to use target points, so-called waypoints, to indicate where the MAV have to go. Among the important aspects of the MAVs in such applications, two of them are the stabilizing performance during the task, and the robust guidance of the vehicle along a desired trajectory. The first has been investigated in many works in the last years (Akbar and Uchiyama, 2017; Zhang and Chen, 2005; Santos and Cunha Jr, 2019; Nemati and Montazeri, 2018), but there are still few papers related to the second one (Shekhar *et al.*, 2015; Santos *et al.*, 2015).

The vehicle dynamic equations are nonlinear and contain the unkown terms, represented by disturbances and uncertanties. The disturbances are mainly caused by wind-structure interactions, while uncertainties represent parametric errors and inaccuracy of the model. Shekhar *et al.* (2015) proposes a model predictive control with variable receding horizon to cope with disturbances and uncertainties, resulting in an effective but complex control algorithm. Santos *et al.* (2015) approaches the waypoint-based position guidance problem for an MAV, which is subject to constant perturbations, is solved using a model predictive controller. Nowadays, with the advance in robust control, particularly on the sliding mode control (SMC) methodology, it is possible to ensure robustness w.r.t. more general disturbances using a simpler approach. However, in a real application of SMC, it is possible to perceive an oscillation with finite frequency and amplitude, the so-called chattering (Lee and Utkin, 2007). This phenomenon is originated by the unmodeled dynamics and discrete-time implementation, being amplified by an excessively large switching gain. Therefore, in the design of the SMC, it is desired to obtain sufficiently large switching gain to compensate the disturbances, but without incurring a high overestimation, which would cause an undesirable level of chattering.

The adaptive sliding mode control problem has been intensively investigated in the last decade (Huang *et al.*, 2008; Lee and Utkin, 2007; Plestan *et al.*, 2010). Such a control method, in which the control gain is obtained by an adaptive law, allows disturbance/uncertainties bounds to be unknown and becomes a suitable choice for practical applications. Hence, a guidance law based on an ASMC technique would guarantee dependability for an MAV subject to unknown disturbance/uncertainties bounds, given stabilizing position and attitude control laws. However, in SMC the system

trajectories have two phases: the reaching and the sliding one. It turns out that the robustness property enssured by the SMC is only valid in the latter phase. In particular, to avoid the reaching phase and provide robustness during all the time, Cong *et al.* (2014) have investigated a time-varying global ASMC formulation.

The present work deals with the waypoints-based guidance of an under-actuated MAV. In this task, the MAV needs to visit all of the specified waypoints in a given sequence. To face the problem, we adopt the hierarchical control structure represented in Fig. 1, in which the guidance is a supervisory outer loop. Furthermore, the stabilizing flight control laws are known and suitably tuned to guarantee that the attitude dynamics are faster than the translation ones. To ensure robustness during all the movement, we adopt the adaptive global sliding mode control (AGSMC) introduced in Cong *et al.* (2014). Using this methodology we can obtain a new robust guidance law with a simpler design than the one in Shekhar *et al.* (2015). Moreover, the guidance law provides appropriate position and heading commands to guarantee the robust tracking performance w.r.t. more general disturbances than the ones considered in (Santos *et al.*, 2015). In summary, the main contributions of the present paper are: 1) the proposal of a waypoint-based guidance structure in which the supervisory loop provides position and heading commands to the stabilizing inner loops; 2) a robust guidance law that makes an under-actuated MAV, subject to disturbances and uncertainties with unknown bounds, visit a specified sequence of waypoints.

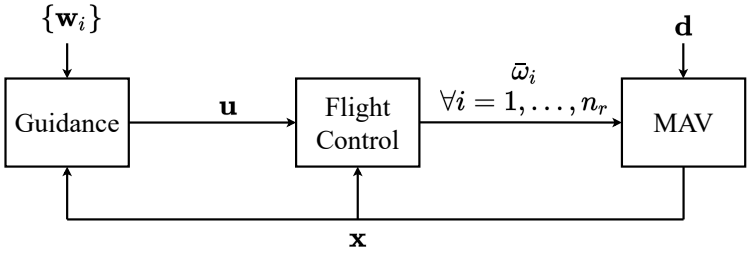

Figure 1. Hierarchical control scheme. $\mathbf{x}$ is the system state, $\mathbf{u}$ is the command provided by the guidance law, $\mathbf{d}$ is the disturbance input, $\{\mathbf{w}_i\}$ is the trackable waypoint sequence, $\bar{\omega}_i$ is the spin command to ith rotor, and n_r is the number of rotors.

The present work is structured as follows. Section 2 presents the mathematical modeling of an under-actuated MAV and defines the paper's main problem. Section 3 formulates the proposed guidance law. Section 4 evaluates the proposed method using computer simulation. Finally, the Section 5 concludes this paper.

2. PROBLEM STATEMENT

This section defines the waypoint-based guidance problem. Subsection 2.1 presents the notation. Subsection 2.3 presents the mathematical modeling of a stabilized under-actuated MAV. Subsection 2.3 defines the paper's main problem.

2.1 Notation

Denote real scalar quantities, column vectors, and matrices by italic lowercase letters, boldface lowercase letters, and boldface uppercase letters, *e.g.*, $a \in \mathbb{R}$, $\mathbf{a} \in \mathbb{R}^n$, and $\mathbf{A} \in \mathbb{R}^{n \times m}$, respectively. Denote the 3×3 identity matrix by $\mathbf{I}_3$ and the standard unit vectors of $\mathbb{R}^3$ by $\mathbf{e}_1 \triangleq (1, 0, 0)$, $\mathbf{e}_2 \triangleq (0, 1, 0)$, and $\mathbf{e}_3 \triangleq (0, 0, 1)$. Denote three-dimensional geometric (Euclidian) vectors by italic lowercase letters with an over arrow, *e.g.*, $\vec{r}$, and three-dimensional points by uppercase letters, such as B. The 2-norm and ∞-norm are denote by $\|.\|$ and $\|.\|_\infty$, respectively. Consider $\mathcal{S}_a \triangleq \{A; \vec{x}_a, \vec{y}_a, \vec{z}_a\}$ to represent a Cartesian coordenate system (CCS), where $\vec{x}_a$, $\vec{y}_a$, and $\vec{z}_a$ are orthonormal geometric vectors with origin at point A. The algebraic vector resulting from the projection of $\vec{r}$ onto $\mathcal{S}_a$ is represented by $\mathbf{r}_a \in \mathbb{R}^3$. The ith component of the vector $\mathbf{r}_a$ is denoted by $r_{a,i}$. Given the vector $\mathbf{r}_a$, we define $\mathbf{r}_{a,i:j}$ as a partition of the $\mathbf{r}_a$, i.e., $\mathbf{r}_{a,i:j} \triangleq (r_{a,i}, \ ..., \ r_{a,j})$. Given the matrix $\mathbf{A}_b$, the component in the ith line and jth column is denoted by $A_{b,ij}$. Moreover, assuming $\mathbf{A}_b$ as a diagonal matrix, we define $\mathbf{A}_{b,i:j} \triangleq \text{diag}\,(A_{ii}, \ ..., \ A_{jj})$. Assuming $\mathcal{S}_b$ as other CCS, the attitude matrix that represents the attitude of $\mathcal{S}_b$ w.r.t. $\mathcal{S}_a$ is denoted by $\mathbf{D}^{b/a} \in \text{SO}(3) \triangleq \{\mathbf{D} \in \mathbb{R}^{3\times3} : \mathbf{D}^{\text{T}}\mathbf{D} = \mathbf{I}_3\}$. An important property of the attitude matrix is $\mathbf{r}_b = \mathbf{D}^{b/a}\mathbf{r}_a$. Finally, consider the vector product $\vec{w} \triangleq \vec{r} \times \vec{v}$. Given the $\mathcal{S}_a$ representations $\mathbf{r}_a$ and $\mathbf{v}_a$ of $\vec{r}$ and $\vec{v}$, respectively, we can compute the $\mathcal{S}_a$ representation $\mathbf{w}_a$ of $\vec{w}$ by $\mathbf{w}_a = [\mathbf{r}_a\times]\mathbf{v}_a$, where $[\mathbf{r}_a\times] \in \mathbb{R}^{3\times3}$ is the skew-symmetric matrix

$$[\mathbf{r}_a\times] \triangleq \begin{bmatrix} 0 & -r_3 & r_2 \\ r_3 & 0 & -r_1 \\ -r_2 & r_1 & 0 \end{bmatrix},$$

with r_1, r_2, and r_3 denoting the components of $\mathbf{r}_a$.

2.2 Mathematical modeling

Consider a Cartesian Coordinate System (CCS) $\mathcal{S}_g \triangleq \{G; \vec{x}_g, \vec{y}_g, \vec{z}_g\}$ fixed on the ground at a known point G, with $\vec{z}_g$ pointing upward vertically. Also consider another CCS $\mathcal{S}_b \triangleq \{B; \vec{x}_b, \vec{y}_b, \vec{z}_b\}$ fixed on the MAV airframe at its center of mass B, with $\vec{x}_b$ pointing forward, and $\vec{z}_b$ pointing upward, normal to the airframe.

The six degrees of freedom (DOF) dynamics of an MAV is commonly described by (Silva Jr and Santos, 2020):

$$\ddot{\mathbf{r}}_g^{b/g} = \frac{1}{m}\mathbf{f}_g^c - g\mathbf{e}_3 + \frac{1}{m}\mathbf{f}_g^d, \tag{1}$$

$$\dot{\mathbf{D}}^{b/g} = -\left[\boldsymbol{\omega}_b^{b/g}\times\right]\mathbf{D}^{b/g}, \tag{2}$$

$$\dot{\boldsymbol{\omega}}_b^{b/g} = \mathbf{J}_b^{-1}\left[\left(\mathbf{J}_b\boldsymbol{\omega}_b^{b/g}\right)\times\right]\boldsymbol{\omega}_b^{b/g} + \mathbf{J}_b^{-1}\left(\boldsymbol{\tau}_b^c + \boldsymbol{\tau}_b^d\right), \tag{3}$$

where $\mathbf{r}_g^{b/g} \in \mathbb{R}^3$ is the $\mathcal{S}_g$ representation of the position vector of $\mathcal{S}_b$ w.r.t. $\mathcal{S}_g$, $m \in \mathbb{R}+$ denotes the mass of the MAV, $g \in \mathbb{R}_+$ denotes the gravity acceleration, $\mathbf{f}_g^c \in \mathbb{R}^3$ and $\mathbf{f}_g^d \in \mathbb{R}^3$ are the $\mathcal{S}_g$ representations of the control and disturbance forces, respectively, $\mathbf{D}^{b/g} \in \mathrm{SO(3)}$ is the attitude matrix of $\mathcal{S}_b$ w.r.t $\mathcal{S}_g$, $\boldsymbol{\omega}_b^{b/g} \in \mathbb{R}^3$ denotes the $\mathcal{S}_b$ representation of the angular velocity of $\mathcal{S}_b$ w.r.t. $\mathcal{S}_g$, $\mathbf{J}_b \in \mathbb{R}^{3\times3}$ denotes the $\mathcal{S}_b$ representation of the airframe inertia matrix, and $\boldsymbol{\tau}_b^c \in \mathbb{R}^3$ and $\boldsymbol{\tau}_b^d \in \mathbb{R}^3$ are the control and disturbance torques, respectively.

The MAVs considered here are equipped with fixed (not vectoring and constant-pitch) and parallel rotors. Therefore, they possess under-actuated dynamics that can produce four independent control inputs (torque in $\vec{x}_b$,$\vec{y}_b$, and $\vec{z}_b$, and force in $\vec{z}_b$). To deal with such unde-actuated dynamics, we adopt a well-known hierarchical flight control structure in which the attitude control is nested inside of the position control loop (Silva Jr and Santos, 2020; Santos and Cunha Jr, 2019). Moreover, assuming that there is a time-scale separation between these two loops, in which the former is much faster than latter, the attitude and position control laws can be designed separately (Silva Jr and Santos, 2020).

The adopted stabilizing attitude and position control laws are, respectively (Santos and Cunha Jr, 2019):

$$\bar{\boldsymbol{\tau}}_b^c = -\mathbf{J}_b\left(\mathbf{K}_1\tilde{\boldsymbol{\alpha}} + \mathbf{K}_2\boldsymbol{\omega}_b^{b/g} + \mathbf{J}_b^{-1}\left[\left(\mathbf{J}_b\boldsymbol{\omega}_b^{b/g}\right)\times\right]\boldsymbol{\omega}_b^{b/g}\right), \tag{4}$$

$$\bar{\mathbf{f}}_g^c = -m\left(\mathbf{K}_3\left(\mathbf{r}_g^{b/g} - \bar{\mathbf{r}}_g^{b/g}\right) + \mathbf{K}_4\dot{\mathbf{r}}_g^{b/g} - g\mathbf{e}_3\right), \tag{5}$$

where $\bar{\boldsymbol{\tau}}_b^c \in \mathbb{R}^3$ is the $\mathcal{S}_b$ representation of the control torque command, $\bar{\mathbf{f}}_g^c \in \mathbb{R}^3$ is the $\mathcal{S}_g$ representation of the control force command, $\mathbf{K}_1 \in \mathbb{R}^{3\times3}$, $\mathbf{K}_2 \in \mathbb{R}^{3\times3}$, $\mathbf{K}_3 \in \mathbb{R}^{3\times3}$, and $\mathbf{K}_4 \in \mathbb{R}^{3\times3}$ are positive-definite diagonal matrices of the tuning parameters, $\bar{\mathbf{r}}_g^{b/g} \in \mathbb{R}^3$ is the $\mathcal{S}_g$ representation of the position command, $\tilde{\boldsymbol{\alpha}} \in \mathbb{R}^3$ contains the 1-2-3 Euler angles corresponding to the attitude error $\tilde{\mathbf{D}} \triangleq \mathbf{D}^{b/\bar{b}} \in \mathrm{SO(3)}$, and $\tilde{\boldsymbol{\omega}} \triangleq \boldsymbol{\omega}_b^{b/\bar{b}} \in \mathbb{R}^3$ is the $\mathcal{S}_b$ representation of the angular velocity error; $\mathcal{S}_{\bar{b}}$ represents the desired pose of $\mathcal{S}_b$.

The time-scale separation ensures that the $\vec{x}_b$–$\vec{y}_b$ plane converges quickly to $\vec{x}_{\bar{b}}$–$\vec{y}_{\bar{b}}$ and, therefore, we can consider that $\tilde{\omega}_1 = \tilde{\omega}_2 = 0$. Moreover, assuming that α_1 and α_2 are small and defining $\delta\mathbf{f} \triangleq \mathbf{f}_g - \bar{\mathbf{f}}_g$ and $\delta\boldsymbol{\tau} \triangleq \boldsymbol{\tau}_b^c - \bar{\boldsymbol{\tau}}_b^c$, by replacing (4)–(5) into (1)–(3), we can obtain the following four-DOF closed-loop model:

$$\ddot{\mathbf{r}}_g^{b/g} = -\mathbf{K}_3\mathbf{r}_g^{b/g} - \mathbf{K}_4\dot{\mathbf{r}}_g^{b/g} + \mathbf{K}_3\left(\bar{\mathbf{r}}_g^{b/g} + \boldsymbol{\gamma}\right), \tag{6}$$

$$\ddot{\psi} = -K_{1,33}\psi - K_{2,33}\dot{\psi} + K_{1,33}\left(\bar{\psi} + \beta\right), \tag{7}$$

where $\boldsymbol{\gamma} \triangleq \mathbf{K}_3^{-1}\left(\mathbf{f}_g^d + \delta\mathbf{f}\right)/m \in \mathbb{R}^3$ and $\beta \triangleq \left(\tau_3^d + \delta\tau_3\right)/\left(K_{1,33}J_{b,33}\right) \in \mathbb{R}$ denote the disturbance/uncertainty forces and torques, respectively.

2.3 Guidance objective

Consider the following definition of waypoints as well as of a waypoint sequence.

Definition 1. Define the ith waypoint $\mathbf{w}_i \in \mathbb{R}^4$ as a vector of three-dimensional position and heading, as well as the sequence of waypoints $\{\mathbf{w}_1,\ \mathbf{w}_2,\ ...,\ \mathbf{w}_{n_p}\}$, where n_p is the number of waypoints.

The main problem of the present paper is enunciated below.

Problem 1. The problem is to design a supervisory outer loop waypoint-based guidance for a stabilized under-actuated MAV described by (6)–(7) so as to robustly conduct it to visit the neighborhood of the waypoints of a given sequence $\{\mathbf{w}_1,\ \mathbf{w}_2,\ ...,\ \mathbf{w}_{n_p}\}$.

3. GUIDANCE LAW STRATEGY

We know that $(\bar{\alpha}_1, \bar{\alpha}_2)$ depends on $\bar{\mathbf{r}}_{g,1:2}^{b/g}$ and, by applying a conventional AGSMC that provides a discontinuous $\bar{\mathbf{r}}_{g,1:2}^{b/g}$, the analyzed system violate the assumed time-scale separation, since $(\bar{\alpha}_1, \bar{\alpha}_2)$ presents a high frequency. Therefore, in this paper we use a partitioned formulation of the guidance law, in which $\bar{\mathbf{r}}_{g,1:2}^{b/g}$ is obtained by a quasi-AGSMC. The commands $\bar{r}_{g,3}^{b/g}$ and $\bar{\psi}$ are obtained by an AGSMC, with independent switching gains.

Let us define the guidance errors as

$$
\begin{aligned}
\mathbf{x}_1 &\triangleq \mathbf{r}_{g,1:2}^{b/g} - \boldsymbol{\eta}_{1:2} \in \mathbb{R}^2, \\
\mathbf{x}_2 &\triangleq \dot{\mathbf{r}}_{g,1:2}^{b/g} - \dot{\boldsymbol{\eta}}_{1:2} \in \mathbb{R}^2, \\
x_3 &\triangleq r_{g,3}^{b/g} - \eta_3 \in \mathbb{R}, \\
x_4 &\triangleq \dot{r}_{g,3}^{b/g} - \dot{\eta}_3 \in \mathbb{R}, \\
x_5 &\triangleq \psi - \eta_4 \in \mathbb{R}, \\
x_6 &\triangleq \dot{\psi} - \dot{\eta}_4 \in \mathbb{R},
\end{aligned}
$$

where $\boldsymbol{\eta} \in \mathbb{R}^4$ is the output of a third-order reference low-pass filter, which we use to provides a smooth command trajectory. Consider Eq. (6)–(7) rewritten in the following state-space form:

$$\dot{\mathbf{x}}_1 = \mathbf{f}_1(\mathbf{x}), \tag{8}$$
$$\dot{\mathbf{x}}_2 = \mathbf{f}_2(\mathbf{x}) + \mathbf{B}_1(\mathbf{u}_{1:2} + \mathbf{d}_{1:2}), \tag{9}$$
$$\dot{x}_3 = f_3(\mathbf{x}), \tag{10}$$
$$\dot{x}_4 = f_4(\mathbf{x}) + B_2(u_3 + d_3), \tag{11}$$
$$\dot{x}_5 = f_5(\mathbf{x}), \tag{12}$$
$$\dot{x}_6 = f_6(\mathbf{x}) + B_3(u_4 + d_4), \tag{13}$$

where $\mathbf{x} \triangleq (\mathbf{x}_1,\ \mathbf{x}_2,\ x_3,\ x_4,\ x_5,\ x_6) \in \mathbb{R}^8$ is the system state, $\mathbf{u} \triangleq (\bar{\mathbf{r}}_g^{b/g},\ \bar{\psi}) \in \mathbb{R}^4$ is the control input, $\mathbf{d} \triangleq (\boldsymbol{\gamma},\ \beta) \in \mathbb{R}^4$ is the disturbance input, $\mathbf{B}_1 \in \mathbb{R}^{2\times 2}$ is a known matrix, $B_2 \in \mathbb{R}$, and $B_3 \in \mathbb{R}$ are known constants, and $\mathbf{f}_1 : \mathbb{R}^8 \to \mathbb{R}^2$, $\mathbf{f}_2 : \mathbb{R}^8 \to \mathbb{R}^2$, $f_3 : \mathbb{R}^8 \to \mathbb{R}^1$, $f_4 : \mathbb{R}^8 \to \mathbb{R}^1$, $f_5 : \mathbb{R}^8 \to \mathbb{R}^1$, $f_6 : \mathbb{R}^8 \to \mathbb{R}^1$ are known functions. The parameters $\mathbf{B}_1$, B_2, B_3, as well as the functions $\mathbf{f}_1$, $\mathbf{f}_2$, f_3, f_4, f_5, and f_6 are given by

$$
\begin{aligned}
\mathbf{B}_1 &\triangleq \mathbf{K}_{3,1:2}, \\
B_2 &\triangleq K_{3,33}, \\
B_3 &\triangleq K_{1,33}, \\
\mathbf{f}_1(\mathbf{x}) &\triangleq \mathbf{x}_2, \\
\mathbf{f}_2(\mathbf{x}) &\triangleq -\mathbf{K}_{3,1:2}\mathbf{x}_1 - \mathbf{K}_{4,1:2}\mathbf{x}_2 - \mathbf{K}_{3,1:2}\boldsymbol{\eta}_{1:2} - \mathbf{K}_{4,1:2}\dot{\boldsymbol{\eta}}_{1:2} - \ddot{\boldsymbol{\eta}}_{1:2}, \\
f_3(\mathbf{x}) &\triangleq x_4, \\
f_4(\mathbf{x}) &\triangleq -K_{3,33}x_3 - K_{4,33}x_4 - K_{3,33}\eta_3 - K_{4,33}\dot{\eta}_3 - \ddot{\eta}_3, \\
f_5(\mathbf{x}) &\triangleq x_6, \\
f_6(\mathbf{x}) &\triangleq -K_{1,33}x_5 - K_{2,33}x_6 - K_{1,33}\eta_4 - K_{2,33}\dot{\eta}_4 - \ddot{\eta}_4.
\end{aligned}
$$

Assume that $\|\mathbf{d}\| \leq \rho < \infty$, with unknown ρ.

3.1 Multi-input AGSMC formulation

Consider the sliding variables (Cong *et al.*, 2014):

$$\mathbf{s}_1(t) \triangleq \boldsymbol{\sigma}_1(t) - \mathbf{P}_1(t)\,\boldsymbol{\sigma}_1(0) \in \mathbb{R}^2, \tag{14}$$
$$s_2(t) \triangleq \sigma_2(t) - P_2(t)\,\sigma_2(0) \in \mathbb{R}, \tag{15}$$
$$s_3(t) \triangleq \sigma_3(t) - P_3(t)\,\sigma_3(0) \in \mathbb{R}, \tag{16}$$

where

$$\boldsymbol{\sigma}_1(t) \triangleq \mathbf{C}_1\mathbf{x}_1 + \mathbf{f}_1(\mathbf{x}) \in \mathbb{R}^2,$$
$$\sigma_2(t) \triangleq C_2 x_3 + f_3(\mathbf{x}) \in \mathbb{R},$$
$$\sigma_3(t) \triangleq C_3 x_5 + f_5(\mathbf{x}) \in \mathbb{R},$$

with $\mathbf{C}_1 \in \mathbb{R}^{2\times 2}$, $C_2 \in \mathbb{R}$, $C_3 \in \mathbb{R}$ representing some constant parameters, and

$$\mathbf{P}_1(t) \triangleq e^{-\lambda_1 t}\mathbf{I}_2 \in \mathbb{R}^{4\times 4},$$
$$P_2(t) \triangleq e^{-\lambda_2 t} \in \mathbb{R},$$
$$P_3(t) \triangleq e^{-\lambda_3 t} \in \mathbb{R},$$

where $\lambda_1, \lambda_2, \lambda_3 > 0$.

Lemma 1 (Exponential stability). If there exists a guidance law $\mathbf{u}$ that makes $(\mathbf{s}_1(t),\ s_2(t),\ s_3(t)) = (\mathbf{0}_{2\times 1},\ 0,\ 0)$, $\forall t \geq t_s$, then the system described by (8)–(13) has a globally exponentially stable equilibrium point at $\mathbf{x} = \mathbf{0}_{8\times 1}$.

Proof. Replacing (8)–(13) and $(\mathbf{s}_1(t),\ s_2(t),\ s_3(t)) = (\mathbf{0}_{2\times 1},\ 0,\ 0)$ into (14)–(16), we obtain:

$$\dot{\mathbf{x}}_1 = -\mathbf{C}_1\mathbf{x}_1 + \mathbf{P}_1(t)\boldsymbol{\sigma}_1(0), \tag{17}$$
$$\dot{x}_3 = -C_2 x_3 + P_2(t)\sigma_2(0), \tag{18}$$
$$\dot{x}_5 = -C_3 x_5 + P_3(t)\sigma_3(0). \tag{19}$$

We know that, by definition, $\mathbf{P}_1(t) \to \mathbf{0}_{4\times 4}$, $P_2(t) \to 0$, $P_3(t) \to 0$ as $t \to \infty$ and, if $\mathbf{C}_1,\ C_2,\ C_3 > 0$, then $(\mathbf{x}_1,\ x_3,\ x_5) = (\mathbf{0}_{2\times 1},\ 0,\ 0)$ is a globally exponentially stable equilibrium point of (8)–(13). Moreover, if $(\mathbf{x}_1,\ x_3,\ x_5) \to (\mathbf{0}_{2\times 1},\ 0,\ 0)$ as $t \to \infty$, then $(\dot{\mathbf{x}}_1,\ \dot{x}_3,\ \dot{x}_5) \to (\mathbf{0}_{2\times 1},\ 0,\ 0)$ as $t \to \infty$ and, therefore, $(\mathbf{x}_2,\ x_4,\ x_6) = (\mathbf{0}_{2\times 1},\ 0,\ 0)$ a is a globally exponentially stable equilibrium point of (8)–(9). □

Now, let us derive a guidance law based on the AGSMC methodology proposed by Cong *et al.* (2014). To address the present multi-input guidance problem, we adopt the unit-vector control strategy (Shtessel *et al.*, 2014) and the adaptation law proposed by Huang *et al.* (2008).

Proposition 1. The guidance law

$$\mathbf{u}_{1-2} = -\left(\frac{\partial \mathbf{f}_1}{\partial \mathbf{x}_2}\mathbf{B}_1\right)^{-1}\left(\left(\mathbf{C}_1 + \frac{\partial \mathbf{f}_1}{\partial \mathbf{x}_1}\right)\mathbf{f}_1 + \frac{\partial \mathbf{f}_1}{\partial \mathbf{x}_2}\mathbf{f}_2 - \dot{\mathbf{P}}_1(t)\boldsymbol{\sigma}_1(0) + \kappa_1(t)\ \text{sat}(\mathbf{s}_1, \varepsilon_1)\right), \tag{20}$$
$$u_3 = -\left(\frac{\partial f_3}{\partial x_4}B_2\right)^{-1}\left(\left(C_2 + \frac{\partial f_3}{\partial x_3}\right)f_3 + \frac{\partial f_3}{\partial x_4}f_4 - \dot{P}_2(t)\sigma_2(0) + \kappa_2(t)\ \text{sign}(s_2)\right), \tag{21}$$
$$u_4 = -\left(\frac{\partial f_5}{\partial x_6}B_3\right)^{-1}\left(\left(C_3 + \frac{\partial f_5}{\partial x_5}\right)f_5 + \frac{\partial f_5}{\partial x_6}f_6 - \dot{P}_3(t)\sigma_3(0) + \kappa_3(t)\ \text{sign}(s_3)\right), \tag{22}$$

with

$$\dot{\kappa}_1(t) = \gamma_1\|\mathbf{s}_1\|H(\|\mathbf{s}_1\| - \varepsilon_1\sqrt{2}), \quad \kappa_1(0) \geq 0, \tag{23}$$
$$\dot{\kappa}_2(t) = \gamma_2|s_2|H(|\mathbf{s}_2| - \varepsilon_2), \quad \kappa_2(0) \geq 0, \tag{24}$$
$$\dot{\kappa}_3(t) = \gamma_3|s_3|H(|\mathbf{s}_3| - \varepsilon_3), \quad \kappa_3(0) \geq 0, \tag{25}$$

where $H(\cdot)$ is the Heaviside function $\gamma_1,\ \gamma_2,\ \gamma_3 > 0$, ensures that $(\mathbf{x}_1,\ \mathbf{x}_2)$ is bounded, $(x_3, x_4, x_5, x_6) \to (0, 0, 0, 0)$, $\kappa_1(t) \to \kappa_{1,max}$, $\kappa_2(t) \to \kappa_{2,max}$, and $\kappa_3(t) \to \kappa_{3,max}$ as $t \to \infty$.

Proof. Assume the Lyapunov candidate function

$$V(\mathbf{s}_1,\ \tilde{\kappa}_1) = \frac{1}{2}\left(\|\mathbf{s}_1\| + |\tilde{\kappa}_1|\right)^2, \tag{26}$$

where $\tilde{\kappa}_1 \triangleq \kappa_1(t) - \kappa_{1,\max}$.

Taking the time derivative of (26), replacing (8)–(13) and (20)–(25) into it, and considering $\|\mathbf{s}_1\| \notin \mathcal{B}(0, \varepsilon_1\sqrt{2})$[1] we obtain

$$\dot{V}(\mathbf{s}_1,\ \tilde{\kappa}_1) \leq -\sqrt{2}\left(\kappa_1(t) - \left\|\frac{\partial \mathbf{f}_1}{\partial \mathbf{x}_2}\mathbf{B}\right\|\rho\right) V^{1/2}, \tag{27}$$

and, therefore, if

$$\kappa_1(t) > \left\|\frac{\partial \mathbf{f}_1}{\partial \mathbf{x}_2}\mathbf{B}\right\|\rho,$$

from the finite-time stability theorem of Bhat and Bernstein (2000), it ensures that $\|\mathbf{s}_1\| \to \mathcal{B}(0, \varepsilon_1\sqrt{2})$ and $\tilde{\kappa}_1 \to 0$ in finite time.

If $\|\mathbf{s}_1\| \in \mathcal{B}(0, \varepsilon_1\sqrt{2})$, $\forall t \geq t_s$, then $\dot{\kappa}_1(t) = 0$ and $\kappa_1(t) = \kappa_{1,max}$, $\forall t \geq t_s$. On the other hand, if $\|\mathbf{s}_1\| \notin \mathcal{B}(0, \varepsilon_1\sqrt{2})$, then the adaptation law (23) makes $\kappa_1(t)$ increase until

$$\kappa_1(t) = \left\|\frac{\partial \mathbf{f}_1}{\partial \mathbf{x}_2}\mathbf{B}\right\|\rho,\ t = t^*.$$

We know that $\rho < \infty$, therefore t^* is also finite. Thus, there exists $t_s = t^* + \Delta t$ in which $\|\mathbf{s}_1\| \in \mathcal{B}(0, \varepsilon_1\sqrt{2})$, $\forall t \geq t_s$, with a finite Δt. Therefore, we have that $\|\mathbf{s}_1\| \to \mathcal{B}(0, \varepsilon_1\sqrt{2})$ and $\kappa_1(t) \to \kappa_{1,max}$ in finite time, with settling time t_s. Moreover, from (14), by knowing that $\dot{\mathbf{x}}_1 = \mathbf{f}_1(\mathbf{x}) = \mathbf{x}_2$, and considering $t \to \infty$, we obtain that $(\mathbf{x}_1,\ \mathbf{x}_2)$ is bounded.

By a analogous development for $|s_2|$ and $|s_3|$, using the Lemma 1, we can prove that $(x_3,\ x_4,\ x_5,\ x_6) \to (0,\ 0,\ 0,\ 0)$, $\kappa_2(t) \to \kappa_{2,max}$, and $\kappa_3(t) \to \kappa_{3,max}$ in finite time. □

Note that there exists a global quasi-sliding mode if and only if the guidance law (20)–(22) and the adaptation laws (23)–(25) ensure that $t_s = 0$. Therefore, the global sliding mode cannot be ensured by the AGSMC proposed by Cong *et al.* (2014) without a priori knowledge about ρ.

4. NUMERICAL SIMULATION

To evaluate the proposed guidance algorithm, we consider an x-shaped quadrotor aerial vehicle with the parameters of Tab. 1. The adopted guidance parameters are $\mathbf{C}_1 = \mathbf{I}_2$, $C_2 = C_3 = 1$, $\lambda_1 = \lambda_2 = \lambda_3 = 1$, $\gamma_1 = \gamma_2 = \gamma_3 = 1$, $\kappa_1(0) = \kappa_2(0) = \kappa_3(0) = 0$, $\varepsilon_1 = 0.081$, $\varepsilon_2 = 0.006$, and $\varepsilon_3 = 0.01$. The control-law parameters are set as $\mathbf{K}_1 = \text{diag}\,(60, 60, 3)$, $\mathbf{K}_2 = \text{diag}\,(15, 15, 4.5)$, $\mathbf{K}_3 = \text{diag}\,(3, 3, 3)$, and $\mathbf{K}_4 = \text{diag}\,(4.5, 4.5, 4.5)$.

Table 1. The parameters of the x-shaped quadrotor aerial vehicle considered in the simulations.

MAV parameters	**Value**
Total mass	1 kg
Inertia matrix	diag(0.015, 0.015, 0.03) kgm^2
Arm length	0.25 m
Half frontal angle	$\pi/4$ rad

The disturbance forces and torques are sinusoidal functions with amplitude of $\|\mathbf{f}_g^d\|_\infty \leq 0.2$ N with frequency $1/2\pi$ Hz, and $\|\boldsymbol{\tau}_b^d\|_\infty \leq 0.01$ N with frequency $1/\pi$ Hz. The specified waypoint sequence is

$$\{\mathbf{w}_i\} = \left\{\begin{bmatrix} 0 \\ 0 \\ 1 \\ \pi/6 \end{bmatrix}, \begin{bmatrix} 0 \\ 1 \\ 1 \\ \pi/6 \end{bmatrix}, \begin{bmatrix} 1 \\ 1 \\ 1 \\ \pi/6 \end{bmatrix}, \begin{bmatrix} 1 \\ 0 \\ 1 \\ \pi/6 \end{bmatrix}, \begin{bmatrix} 1 \\ 0 \\ 0 \\ \pi/6 \end{bmatrix}\right\}.$$

We use the Runge-Kutta 4th-Order solver, with sampling time/integration step $T = 0.01$s. The rotor dynamics, which have not been considered in the control law design, are modeled in the present simulation considering first-order linear models.

[1] $B(\mathbf{y}, r) \subset \mathbb{R}^n$ denotes an open ball with center at $\mathbf{y} \in \mathbb{R}^n$ and radius $r \in \mathbb{R}_+$.

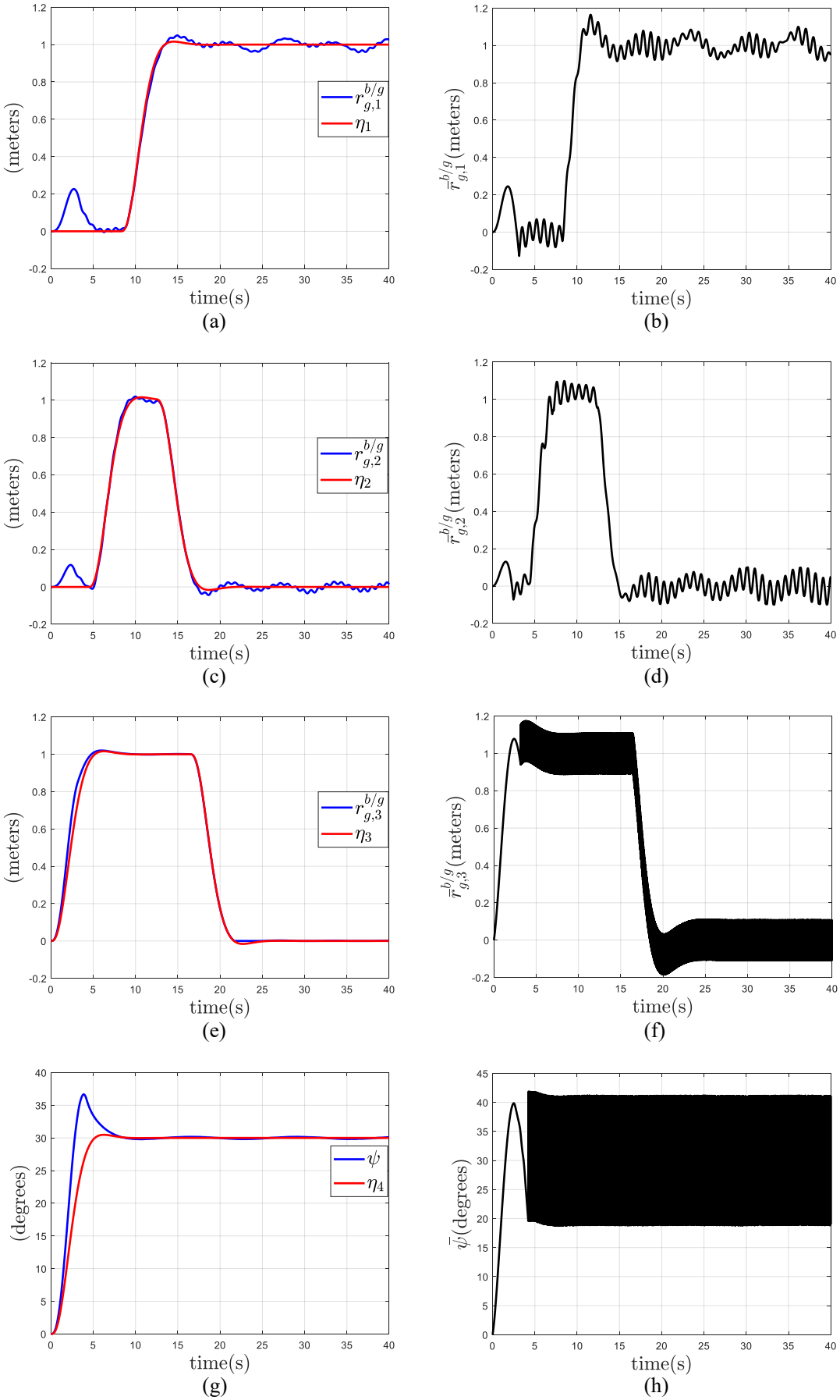

Figure 2. MAV dynamics for three-dimensional position and heading commands.

The results are presented in Figure 2–4. We observe that the quasi-AGSMC provides continuous guidance commands in Fig. 2b and Fig. 2d, and the conventional AGSMC provides discontinuous ones in Fig. 2f and Fig. 2h. However, the signals obtained by the quasi-AGSMC do not provide insensitivity w.r.t. disturbances, since the real trajectories do not match the desired ones, and present a frequency similar to the $\mathbf{f}_g^d$. Moreover, there exists a period, at the beginning of the flight, in which we do not have a switching performance in Fig. 2f and 2h. It indicates that the method proposed by Cong *et al.* (2014) does not provide a global sliding mode to the system.

Note that the AGSMC guidance law provides commands with different dynamics w.r.t. the real trajectory. This difference is related to the disturbance compensation, since the guidance law supplies robustness to the trajectory. Moreover, there is a switching performance in the commands, this results from the adopted SMC methodology. In addition, we obtain all the results considering actuators with first-order linear models and, therefore, the high frequency presented in the guidance commands is acceptable in real applications, since the signals obtained are already subjected to the actuator dynamics.

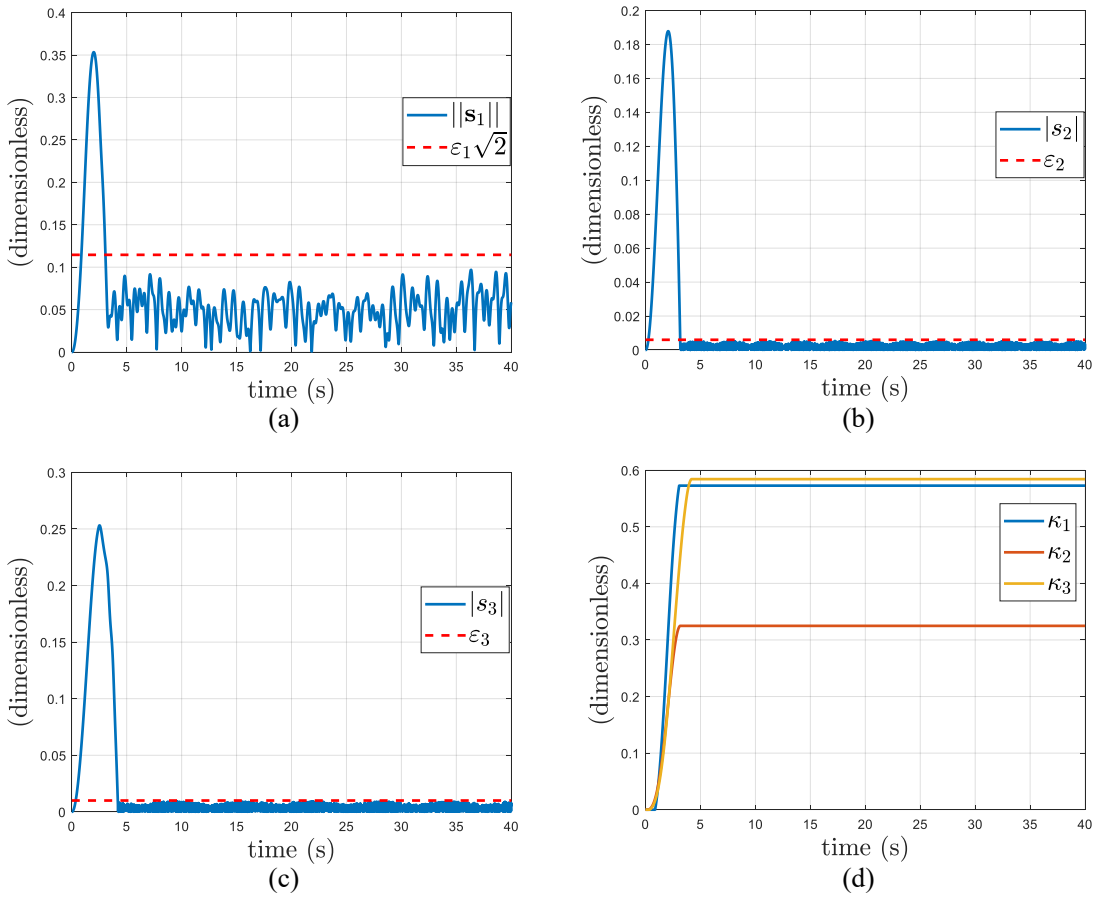

Figure 3. Dynamics of the sliding variables and the switching gains along the flight.

In Fig. 3, we note that the system loses the sliding mode on the adaptation phase of $\kappa_i(t),\ \forall i = 1, 2, 3$ and, therefore, the AGSMC proposed by Cong *et al.* (2014) does not provide a global sliding mode. Moreover, there exists the convergence of $\kappa_i(t),\ i = 1, 2, 3$, and, therefore, the parameters ε_1, ε_2, and ε_3 were suitably chosen. The tuning of ε_1 must be precise, because a small value makes the guidance signal violate the time-scale separation, and a high value increases the sensibility of the system to the disturbances. On the other hand, the values of ε_2 and ε_3 need only to ensure a convergence of $\kappa_2(t)$ and $\kappa_3(t)$, respectively.

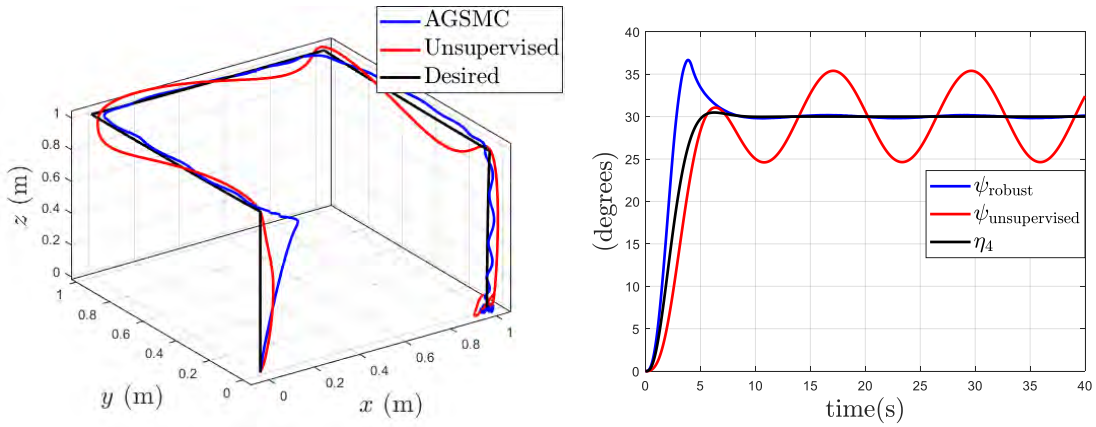

Figure 4. Comparative of the system performance with the AGSMC guidance law and the unsupervised guidance.

From the Fig. 4, we observe that the MAV visits the specified waypoint sequence, but it gets away from the desired trajectory for a brief period of time, between the origin and the first waypoint. This deviation is caused by the adaptation phase of $\kappa_i(t)$ and, as we can see, after the first waypoint the system has a better performance with the proposed guidance law. Therefore, there is a profit with the use of the AGSMC guidance law w.r.t. the unsupervised guidance. However, note that the trajectory obtained by the robust guidance law is not coincident w.r.t. desired trajectory, thanks to the quasi-AGSMC of (20).

5. CONCLUSION

The paper proposed a simple and robust guidance law that makes the MAV visit a specified waypoint sequence. The results presented here do not depend on the amplitude of the waypoints (since there is no assumption about this) and, therefore, are valid for position waypoints with larger values than used in this paper, as long as all assumptions w.r.t. Euler's angles made here are satisfied. In future works, we will use a smooth second-order sliding mode to reduce the sensitivity of the MAV w.r.t disturbances without violating the time-scale separation. Moreover, this guidance law will be evaluated with a flight experiment in an indoor arena equipped with a motion capture system.

6. ACKNOWLEDGEMENTS

The authors would like to thank the Sao Paulo Research Foundation (FAPESP) for the financial support (grant 2019/05334-0). The third author is also grateful for the support of CNPq/Brazil (grant 302637/2018-4).

7. REFERENCES

Akbar, R. and Uchiyama, N., 2017. "Adaptive modified super-twisting control for a quadrotor helicopter with a nonlinear sliding surface". In *2017 SICE International Symposium on Control Systems (SICE ISCS)*. IEEE, pp. 1–6.

Bhat, S.P. and Bernstein, D.S., 2000. "Finite-time stability of continuous autonomous systems". *SIAM Journal on Control and Optimization*, Vol. 38, No. 3, pp. 751–766. doi:10.1137/s0363012997321358.

Cong, B.L., Chen, Z. and Liu, X.D., 2014. "On adaptive sliding mode control without switching gain overestimation". *International Journal of Robust and Nonlinear Control*, Vol. 24, No. 3, pp. 515–531. doi:10.1002/rnc.2902.

Huang, Y.J., Kuo, T.C. and Chang, S.H., 2008. "Adaptive sliding-mode control for Nonlinear Systems with uncertain parameters". *IEEE Transactions on Systems, Man, and Cybernetics, Part B (Cybernetics)*, Vol. 38, No. 2, pp. 534–539.

Lee, H. and Utkin, V.I., 2007. "Chattering suppression methods in sliding mode control systems". *Annual Reviews in Control*, Vol. 31, No. 2, pp. 179–188. doi:10.1016/j.arcontrol.2007.08.001.

Nemati, H. and Montazeri, A., 2018. "Analysis and design of a multi-channel time-varying sliding mode controller and its application in unmanned aerial vehicles". *IFAC-PapersOnLine*, Vol. 51, No. 22, pp. 244–249. doi: 10.1016/j.ifacol.2018.11.549.

Park, S., Zhang, L. and Chakraborty, S., 2016. "Design space exploration of drone infrastructure for large-scale delivery services". In *Proceedings of the 35th International Conference on Computer-Aided Design*. ACM.

Plestan, F., Shtessel, Y., Brégeault, V. and Poznyak, A., 2010. "New methodologies for adaptive sliding mode control". *International Journal of Control*, Vol. 83, No. 9, pp. 1907–1919. doi:10.1080/00207179.2010.501385.

Rajendran, S. and Srinivas, S., 2020. "Air taxi service for urban mobility: A critical review of recent developments, future challenges, and opportunities". *Transportation Research Part E: Logistics and Transportation Review*, Vol. 143, p.

102090.

Santos, D.A. and Cunha Jr, A., 2019. "Flight control of a hexa-rotor airship: Uncertainty quantification for a range of temperature and pressure conditions". *ISA transactions*, Vol. 93, pp. 268–279.

Santos, D.A., Prado, I.A.A. and Bezerra, J.A., 2015. "Waypoint-based guidance with obstacle avoidance for multirotor vehicles using a model predictive controller". In *23rd ABCM International Congress on Mechanical Engineering*.

Shekhar, R.C., Kearney, M. and Shames, I., 2015. "Robust model predictive control of unmanned aerial vehicles using waysets". *Journal of Guidance, Control, and Dynamics*, Vol. 38, No. 10, pp. 1898–1907. doi:10.2514/1.g000787.

Shtessel, Y., Edwards, C., Fridman, L. and Levant, A., 2014. *Sliding mode control and observation*. Springer.

Silva Jr, A.L. and Santos, D.A., 2020. "Fast nonsingular terminal sliding mode flight control for multirotor aerial vehicles". *IEEE Transactions on Aerospace and Electronic Systems*, pp. 4288–4299.

Zhang, S. and Chen, C., 2005. "Backstepping based nonlinear integral sliding mode control for quadrotors under external disturbances". In *2019 Chinese Control Conference (CCC)*. IEEE. doi:10.23919/chicc.2019.8865215.

8. RESPONSIBILITY NOTICE

The authors are solely responsible for the printed material included in this paper.